Supplement of The Cryosphere, 16, 2203–2223, 2022
https://doi.org/10.5194/tc-16-2203-2022-supplement

The Cryosphere
Open Access

Supplement of

Resolving glacial isostatic adjustment (GIA) in response to modern and future ice loss at marine grounding lines in West Antarctica

Jeannette Xiu Wen Wan et al.

Correspondence to: Natalya Gomez (natalya.gomez@mcgill.ca)

S1 GIA modelling setup considerations

Here we briefly explore the influence of model setup factors that impact the predicted GIA, namely: input load resolution, GIA model resolution, and loading changes outside the region of interest. We use the ICE-RD model to explore these issues, which provides ice thickness at 10 km across Antarctica with a region at 1 km resolution over the ASE. From this, we produce an ice model on the GIA model grid in a variety of ways summarised in Table A1. ANT_10km is the 10 km AIS-wide ice sheet model run and ASE_1km is the nested 1km ice sheet model run conducted under the same model forcing and receiving boundary conditions from the continental run. Figure S3.1 shows the ice models ASE_1km and ANT_10km, and corresponding modelled sea level change due to a purely elastic GIA response across the 150-years of ice loss from 1950 to 2100. Figure S3.2 provides an overview of the errors due to different GIA model setup methods (Fig. S3.2d a,b,c) relative to the error from GIA model resolution (Fig. S3.2d).

Ice Model ID	Description
ASE_1km	1 km resolution regional ice sheet model run in ASE
ANT_10km	10 km resolution continental-scale ice sheet model run over all Antarctica
ASE_5km	ASE_1km, downsampled by a factor of 0.2 to achieve a resolution of ~ 5 km
ASE_10km	ANT_10km cropped over region of ASE_1km
ASE_ANT	ASE_1km over ASE, and ANT_10km over rest of Antarctica

Table A1. Overview of the various GIA model setups

Since ASE_1km only covers our region of interest (ROI) the Amundsen Sea Embayment, we first explore the importance of adding the loading pattern outside the ROI using ASE_ANT and ASE_1km (Fig. S3.2a). Comparing simulations with fixed and evolving ice outside the ASE indicate that deformation due to mass changes outside domain of interest result in a broad, superimposed signal of uplift or subsidence. Not considering mass changes outside the region of interest (e.g. Kachuck et al., 2020) can result in a difference in predicted deformation of at least 6% (and up to 50% at the ROI edge) of the overall signal in the region. The implication of this result is that when modelling regional GIA, we must input the surrounding load changes beyond the ROI. The exact bounding region required is outside the scope of this study.

To isolate the effect of using different ice sheet model resolutions, we compared the results of ASE_10km and ASE_1km (Fig. S3.2b). We also explored the effect of using the same load at different resolutions, by resampling the ASE_1km load grid by a factor of 0.2 to result in a 5 km resolution load grid (ASE_5km). We compute the effect of instantaneous removal of the ice load change from 1950 to 2100 and find that calculations of the resulting elastic GIA response are influenced by:

- **Resolution of Dynamic Ice Sheet Model** (Fig S3.2.b): Improving the ice sheet model resolution from 10 km to 2 km (i.e. ANT_10km – ASE_1km) produces SL predictions with up to 40 cm difference. This has the largest effect, because a different ice sheet model resolution will result in different realisations of the ice sheet dynamics (i.e. a different load in the GIA model).

- **Load Resolution** (Fig. S3.2c): Between a 1 km and 5 km resolution load grid of the same forcings (i.e. ASE_1km – ASE_5km) we find up to 14 cm difference in SL predictions, with the largest error along the load edge (i.e. grounding line).
- **GIA Model Grid Resolution** (Fig. S3.2d): For the ice model ASE_1km, improving the GIA model resolution from 7.5 km to 1.9 km produces SL predictions with up to 16 cm difference.

Results from Figure S3.2 indicate that refining the GIA model grid resolution from 7.5 to 1.9 km has a similar effect as refining of the input ice load resolution. The effect of load and GIA model resolution both have a predictable pattern whereby the largest error occurs along the load edges. Accordingly, we recommend efforts in improvements in GIA model accuracy go towards constraining the wavelength of ice cover changes, and improving the resolution of the ice model (i.e. ice sheet observations and models) accordingly. The load set up, including interpolation techniques and consideration of the load outside the ROI are also important.

S2 Viscosity variations scaling factor

This section aims to provide further detail on the scaling factor used to set viscosity variations in our 3-D GIA model and how our scaling factor values compare with results in past literature. We direct readers to the references herein for a complete understanding of the background theory and methodology. As discussed in the main text, 3-D mantle viscosity variability in our Earth models is derived from seismic velocity data by scaling shear wave velocity anomalies to viscosity variability using the method described in Ivins and Sammis (1995) and Kaufmann et al. (2005). We adopt the more streamlined approach in e.g. Austermann et al (2013) that results in an exponential scaling factor, ϵ, which controls lateral viscosity variations. This scaling factor is often chosen empirically to realize a certain expected viscosity variation range with the values ϵ = [0.005 - 0.04] 1/K for all depths. It follows immediately from Kaufmann et al, 2005 (eq. 8) that

$$\epsilon = \epsilon(r) - (E + pV)/(R * T_o^2)$$

Adopting tabulated Earth properties of activation energy and background temperature T_o for the whole mantle convection from Kaufmann at el, 2005, it is possible to extend ϵ into an equivalent scaling function with the surface value of 0.02071 K^{-1}, slowly decreasing from the depth of 300 km towards the CMB to take the value of 0.01625 K^{-1}. A hybrid approach is then to write

$$\epsilon = \epsilon_{surf} * F(r)$$

where F(r) is a normalized function of depth ranging from 1 (first 300 km) to 0.785 (CMB) and ϵ_{surf} is a "free" scaling factor. Setting ϵ_{surf} = 0.02071 K^{-1} brings our EM1_M scaling factors in full agreement with Kaufmann et al. (2005).

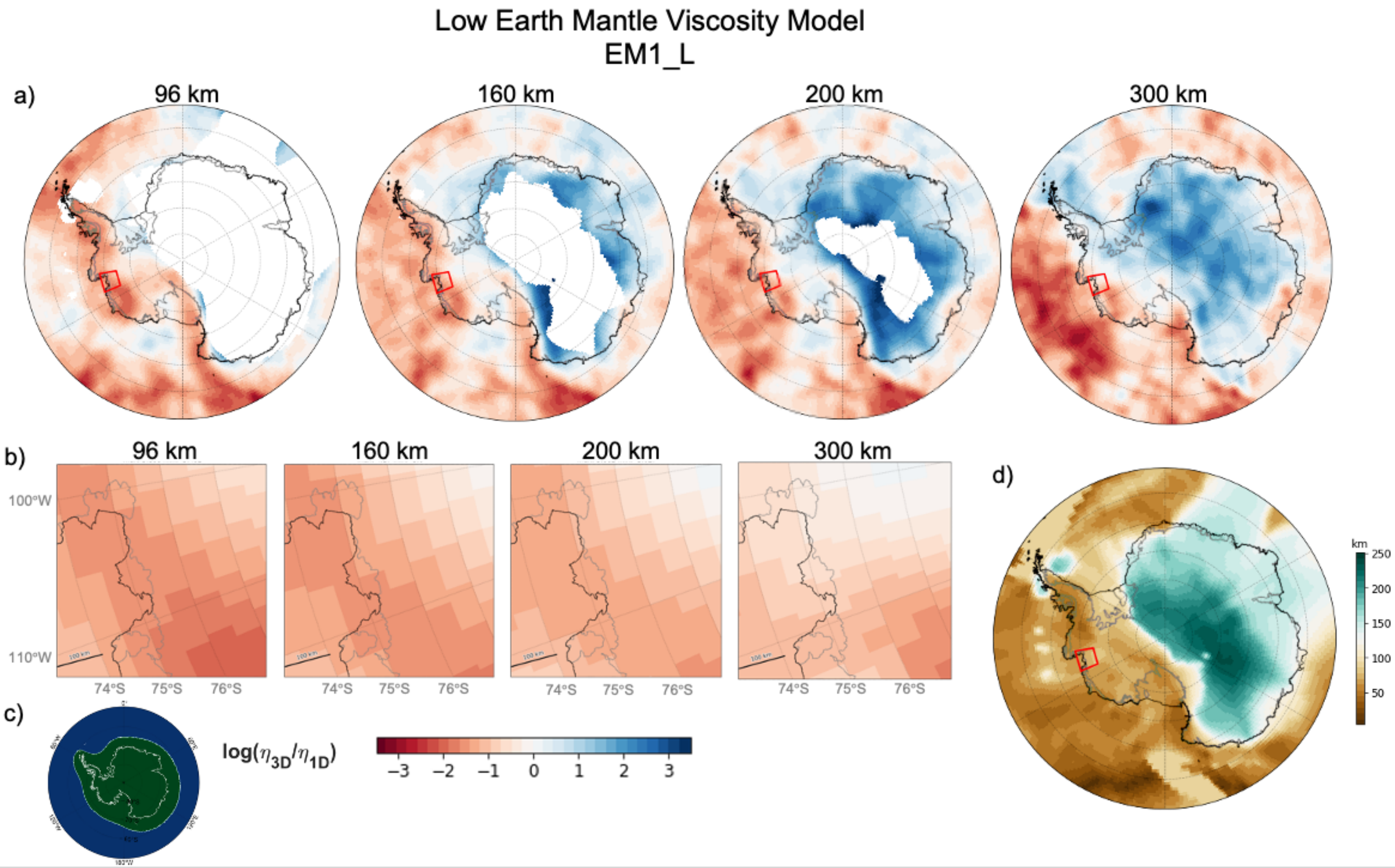

Figure S1. Earth Model Summary. Logarithmic viscosity perturbation map of at depths 96, 160, 200, and 300 km for low Earth mantle viscosity model EM1_L over (a) Antarctica; (b) study region in the Amundsen Sea Embayment. Values are relative to reference 1-D model with upper mantle viscosity of 1 x 1020 Pa s, and lower mantle viscosity of 5 x 1021 Pa s. The black line delimits the edge of the Antarctic ice shelf including the extent of marine-based ice, and the gray line shows the location of the grounding line from Bedmap2 (Fretwell et al., 2013). (c) Regions in the mantle viscosity model. Green region is where regional seismic model ANT20 (Lloyd et al., 2020) data is used; Blue region (global) is where global seismic tomography model S362ANI (Kustowski et al., 2018) data is used. (d) Elastic lithospheric thickness (km) across Antarctica based on the model by An et al. 2015, scaled to produce a regional average lithospheric thickness of 96 km.

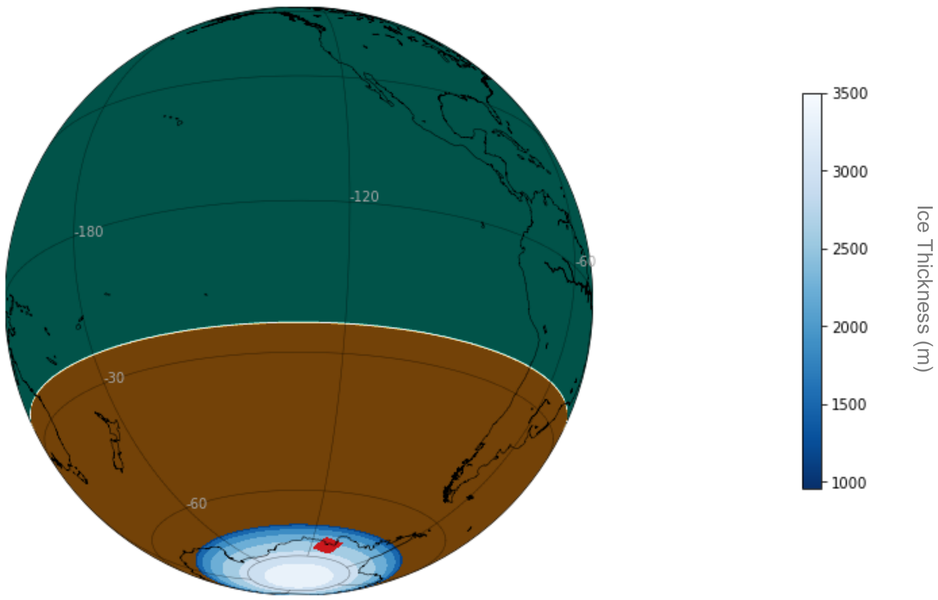

Figure S2. Topography and ice model setup for idealised experiments. The idealised simulations presented in Section 3 are performed with an idealized topography of 3800 m south of 24.5 °S (brown) and - 835 m everywhere else (turquoise) to reflect the 30:70 land to sea ratio on Earth. Over Antarctica, a radially symmetric ice sheet with steady-state Antarctic ice dome profile (Paterson and Colbeck, 1980) sits on top of this topography extending from the south pole to 69 °S, with a maximum height of 3500 m. The colour bar represents the ice thickness of this ice sheet. The red box represents the ASE location of focus in this study.

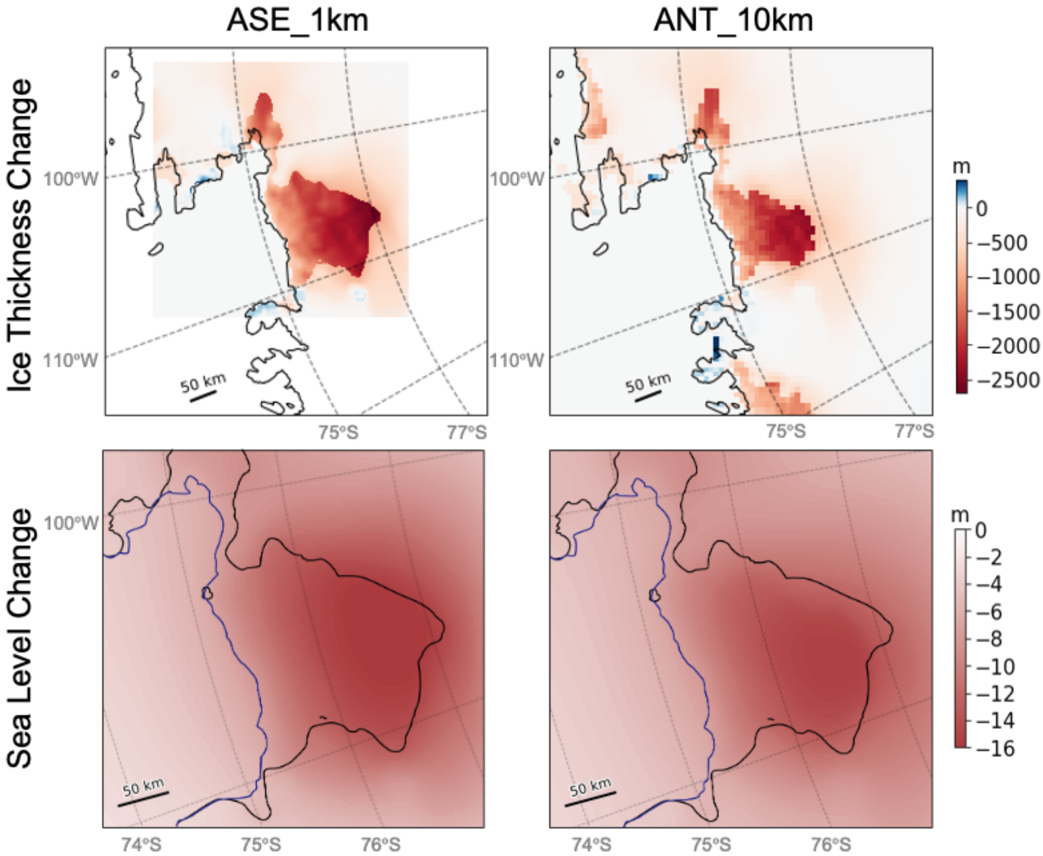

Figure S3.1. ASE_1km and ANT_10km ice model load change between 1950 to 2100, and resulting sea level change due to elastic GIA response.

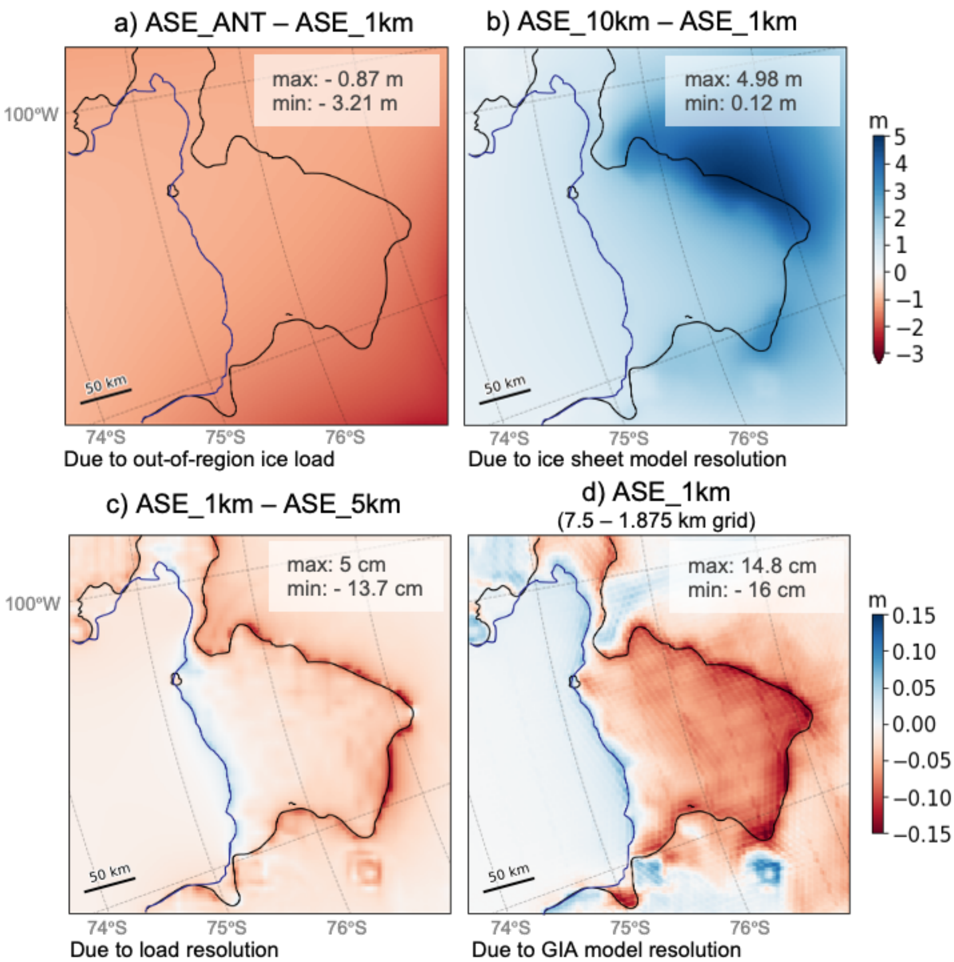

Figure S3.2. Difference in predicted sea level change (m) between 1950 to 2100 from elastic GIA runs of various ice load configurations (Table S1). Each frame represents the difference in GIA predictions due to a) out of region ice loading, b) ice sheet model resolution, c) load resolution and d) GIA model resolution.